Mon. Not. R. Astron. Soc. **268,** L29–L34 (1994)

The shock-excited P Cygni nebula

M. J. Barlow,[1] J. E. Drew,[2] J. Meaburn[3] and R. M. Massey[3]

[1] *Department of Physics & Astronomy, University College London, Gower Street, London WC1E 6BT*
[2] *Department of Physics, University of Oxford, Keble Road, Oxford OX1 3RH*
[3] *Department of Physics & Astronomy, The University, Manchester M13 9PL*

Accepted 1994 March 4. Received 1994 January 6

ABSTRACT

We have obtained images in the [N II] λ6584 line of the nebula around the luminous blue variable star P Cygni, using a 4 arcsec wide occulting strip. A nearly circular inner nebula is found, containing many bright condensations, with angular diameters of 21.4 arcsec in the east–west direction and 23.8 arcsec in the north–south direction. Two fainter outer arcs of [N II] emission are also visible, with angular diameters of 1 and 1.5 arcmin. A high-resolution 4900–9000 Å UES spectrum, obtained at a position 9 arcsec west of P Cygni, shows the [Ni II] λλ7378, 7412 doublet to be the strongest feature emitted by the nebula. High-resolution long-slit MES spectra were obtained at multiple positions across the bright inner nebula in order to investigate the density, dynamics and age of the nebula. Our [N II] λ6584 spectra show broad velocity components with an overall expansion velocity of 140 km s^{-1}, while our [Ni II] λ7412 spectra show much narrower velocity components with an overall expansion velocity of only 110 km s^{-1}. Our results are consistent with the narrow [Ni II] emission originating from dense, mainly neutral knots which are being overtaken by the stellar wind from P Cyg at a relative velocity of 100 km s^{-1}, with the broader irregular [N II] and [S II] emission arising from bow shocks around the knots. This model provides a natural explanation for the larger [N II] expansion velocities compared to those of [Ni II].

Key words: line: profiles – stars: individual: P Cygni – stars: mass-loss – ISM: bubbles.

1 INTRODUCTION

P Cygni, along with η Carinae and S Doradus, is one of a group of stars now known as luminous blue variables (LBVs: Conti 1984; Humphreys 1989; Davidson, Moffat & Lamers 1989). A number of these LBVs have circumstellar nebulae. Abundance analyses of these point to large nitrogen enhancements, indicative of CNO-cycle-processed material removed by mass loss from these massive stars. Examples include the η Carinae homunculus (Davidson et al. 1986), the AG Carinae ring nebula (Mitra & Dufour 1990; Smith 1991; Nota et al. 1992) and the nebulae of a number of LBVs in the Large Magellanic Cloud (Walborn 1982; Stahl & Wolf 1986; Clampin et al. 1993).

P Cygni had appeared to differ from many of the other LBVs in lacking a circumstellar nebula, although Wendker (1982; see also Baars & Wendker 1987) reported an arc of faint thermal radio emission extending about 1 arcmin to the north-east of P Cyg, which had no known optical counterpart at that time. Leitherer & Zickgraf (1987) imaged P Cygni in narrow-band Hα, [N II] 6584-Å and continuum interference filters, finding evidence for excess radial emission in both Hα and [N II] out to about 7-arcsec radius. This was fitted to an r^{-2} density distribution, where r is the distance from the star, and attributed to a stellar wind where matter has been ejected in dense shells.

Johnson et al. (1992; hereafter JBDB) detected nebular emission lines of Hα, [N II], [S II] and [Ni II] in a long-slit spectrum offset 9 arcsec east from P Cygni. The [S II] λλ6717, 6731 doublet ratio yielded a nebular electron density of 600 cm^{-3}, a factor of 20 higher than the value attributable to the expansion of the present-day stellar wind (JBDB). The [N II] and [S II] line fluxes were used to derive an N/S ratio of 33 ± 5 by number, five times larger than solar, implying extensive CN-cycle processing of the material prior to its ejection from the star. An anomalously strong nebular [Ni II] λ6667 line was also discovered by JBDB – its strength too great to be consistent with collisional excitation at the low densities implied by the observed [S II] ratio.

The observations of JBDB were insufficient to define the structure, overall extent or internal dynamics of the P Cygni nebula. We were therefore motivated to obtain imagery and echelle spectroscopy of the nebula in a number of the strongest nebular emission lines.

2 SPECTROSCOPY WITH THE UTRECHT ECHELLE SPECTROGRAPH

On 1992 September 16 UT we obtained an echelle spectrum of the P Cygni nebula at a position offset 9 arcsec due west from P Cyg. The 31.6 line mm^{-1} grating of the Utrecht Echelle Spectrograph (UES), mounted at the Nasmyth focus of the 4.2-m William Herschel Telescope, was used along with an EEV 1251×1152 pixel CCD detector with square 22.5-μm pixels giving 0.33 arcsec $pixel^{-1}$ along the slit. The wavelength coverage from 5000 to 9000 Å was continuous out to 6000 Å, with gaps appearing at longer wavelengths. The 6 arcsec long slit of 0.92-arcsec width was aligned north–south and delivered a resolution of 7 km s^{-1}, as determined from the FWHM of comparison arc lines. Two 600-s exposures were obtained at the offset position. Shorter exposure on-star spectra of P Cyg itself were also obtained. In addition to the expected emission lines of [N II], [S II] and [Ni II], a number of strong [Fe II] lines were detected in our UES nebular spectrum.

Fig. 1(a) shows the profile of the [N II] λ6584 line in our UES offset spectrum, in velocity units, while Figs 1(b) and (c) show the λ7377.83 and the λ7411.71 transitions of [Ni II], the latter having the same upper level as the λ6666.8 line previously observed by JBDB. All the spatial increments along the 6-arcsec slit-length were co-added to produce these spectra. The local standard of rest (LSR) stellar radial velocity was determined to be -22.6 ± 1.5 km s^{-1} from measurement of the on-star [Ni II] λλ7378 and 7412 line profiles. Since these profiles have the flat-topped appearance expected of optically thin lines forming in a constant-velocity outflow, their FWZI of 440 ± 5 km s^{-1} provides a good estimate of twice the wind terminal velocity. Among the nebular profiles shown in Fig. 1, multiple velocity components are particularly prominent in the brighter [Ni II] λ7378 line. The two strongest velocity components in this profile (Fig. 1b) were measured to have FWHM of 18 km s^{-1} and peak-to-peak separations of 110 km s^{-1}. The [N II] nebular profile (Fig. 1a) is considerably less structured, with the strongest components having FWHM in excess of 60 km s^{-1}.

Our on-star spectrum of P Cyg shows a negligible change in instrumental sensitivity between 7378 and 7412 Å. Hence, for the two [Ni II] lines in the offset nebular spectrum (Fig. 1), we derive a line flux ratio $I(7378)/I(7412) = 3.7$. Using the atomic data of Nussbaumer & Storey (1982), the predicted ratio for collisional excitation of these lines, at electron densities between 500 and 10^4 cm^{-3} and any electron temperature in excess of 3000 K, should be between 6 and 16. The predicted ratio for these lines in statistical equilibrium (e.g. at the high-density limit, or if the upper levels are populated by fluorescent cascading) is 1.645. The ratio of the fluxes in these lines in the on-star spectrum is 1.54 ± 0.10. This is in satisfactory agreement with the high-density limit, appropriate to emission from P Cyg's wind. For the case of collisional excitation alone, the observed nebular flux ratio of 3.7 would require an electron density of about 5×10^6 cm^{-3}. As pointed out by JBDB, such a density appears at first sight to be inconsistent with the absence of nebular emission in the [N II] λ5755 line (both in the offset nebular spectrum of JBDB and in our current offset UES spectrum) – this matter is discussed further in Section 5.

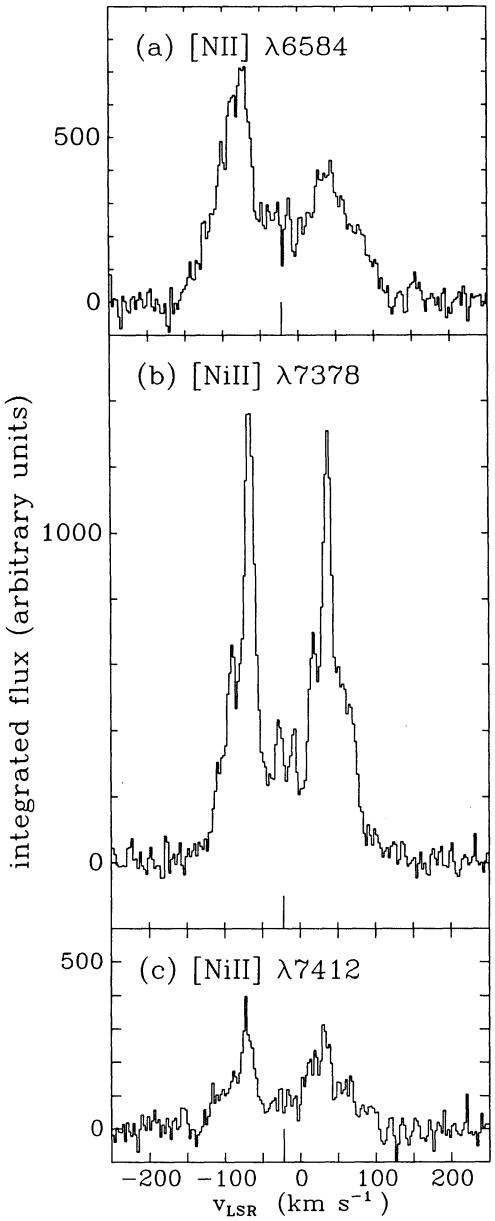

Figure 1. Profiles of the [N II] 6584-Å and [Ni II] 7378, 7412-Å lines obtained at an offset 9 arcsec west of P. Cygni. The three panels share a common velocity scale (referred to the local standard of rest). The flux scales have been set such that ratios between the areas under the plotted profiles reflect the observed flux ratios. The radial velocity of P Cygni is indicated by an extended tick-mark on the velocity axis.

At their 9 arcsec east position, JBDB found [N II] λ6584 to have a dereddened flux of 283, on a scale where Hα is 285. We cannot easily measure the nebular Hα emission in our UES spectrum, and so assume that [N II] has the same relative strength of 283 at the 9 arcsec west position. We measured the equivalent widths of nebular emission lines in our offset UES spectrum relative to the strength of the on-star continuum, and normalized these equivalent widths to an 18 000-K, $\log g = 2.05$ Kurucz model atmosphere which Deacon & Barlow (1991) found to provide a good fit to the dereddened ultraviolet and optical energy distribution of P Cyg. With the relative strength of [N II] λ6584 set to 283,

[Ni II] λλ7378 and 7412 are found to have strengths of 403 and 108, respectively. Some nebular [O III] λ5007 emission was also found to be present, with a relative strength of 110^{+20}_{-50}.

3 NARROW-BAND IMAGERY WITH THE MANCHESTER ECHELLE SPECTROMETER

The Manchester Echelle Spectrometer (MES; Meaburn et al. 1984), mounted at the *f*/15 Cassegrain focus of the 2.5-m Isaac Newton Telescope, was used in its direct imaging mode to obtain narrow-bandpass-filter images of the P Cygni nebula. The [N II] imaging observations were carried out on 1993 June 3/4 UT. We used the EEV5 CCD detector, with 1280 × 1180 22.5-μm square pixels which, with 2 × 2 binning, gave a plate scale of 0.255 arcsec pixel^{-1} for the final usable 460 × 350 pixel field (117 × 89 arcsec^2). Because of the extreme brightness of P Cyg ($V = 4.8$), a chromium occulting strip of projected width 4.3 arcsec was centred on the star for all the imaging observations, in order to reduce the central brightness.

To obtain the [N II] nebular images, obervations were made through two filters: a narrow-bandpass filter (10-Å FWHM) centred at 6584 Å, whose purpose was to isolate the nebular emission as much as possible from the scattered stellar emission; and a broader-bandpass filter (90-Å FWHM) centred at 6580 Å. Observations were obtained with the occulting strip aligned north–south and east–west on the sky. For each orientation, three 600-s exposures were obtained through the narrow [N II] filter, followed by a 10-s exposure through the broad [N II] filter. Individual CCD exposures were debiased and cleaned of cosmic ray hits using the Starlink data reduction package FIGARO. The chromium occulting strip was not completely opaque, transmitting about 0.1 per cent of the incident light. This allowed us to align individual exposures accurately to the same central peak. The residual transmission of the central image of P Cyg also allowed us to measure the seeing, which was found to have an average of 0.96 arcsec FWHM during the [N II] observations (the seeing measured from fainter stellar images was 0.8 arcsec). After alignment and normalization of the central stellar peaks in each of the narrow-band and broad-band images obtained at the same orientation, the latter were subtracted from the former to reveal the [N II] nebular emission.

The resultant continuum-subtracted [N II] images are displayed in Figs 2(a) and (b) respectively (opposite p. L32). A nearly circular nebula with a sharp outer boundary and reproducible details is clearly present in both images. The angular diameters of this nebula are 23.8 arcsec in the north–south direction and 21.4 arcsec in the east–west direction. Many bright condensations are present within this nebula, particularly to the north of P Cyg. For a distance to P Cyg of 1.8 kpc (Section 5), the mean nebular radius of 11.3 arcsec corresponds to an absolute radius of 0.099 pc. After calibrating the images against observations of the white dwarf standard Feige 56, we estimate an integrated [N II] λ6584 flux of $(1.7 \pm 0.3) \times 10^{-12}$ erg cm^{-2} s^{-1}. This includes an assumption that 16 per cent of the total emission was hidden by the 4.3 arcsec wide occulting strip.

In Figs 3(a) and (b) (opposite p. L32) the full fields of view of the narrow-band [N II] images are shown. Note that the scattered stellar continuum has not been subtracted from these images. The central regions in these images have been overexposed in order to bring out faint outer nebular emission features. Two outer arcs of emission can be seen in both images, the innermost of the two being prominent to the east and south of P Cyg, with an angular diameter of ~60 arcsec, while an outer arc of emission is also present, particularly to the north, with an angular diameter of ~90 arcsec. There is no obvious correspondence, however, between the outer nebular features observed here and the arc of faint thermal radio emission extending about 1 arcmin to the north-east of P Cyg found by Wendker (1982) and Baars & Wendker (1987). The approximate angular radii of 30 and 45 arcsec for the outer shells correspond to absolute radii of 0.26 and 0.39 pc, respectively, for a distance to P Cyg of 1.8 kpc.

4 LONG-SLIT SPECTROSCOPY WITH THE MANCHESTER ECHELLE SPECTROMETER

We obtained long-slit MES spectra of the P Cygni nebula at the wavelengths of the following lines: [N II] λ6584, [Ni II] λ7412 and the [S II] λλ6717, 6731 density-sensitive doublet. For all observations the slit was oriented east–west with a slit-width of 150 μm, which projected to 0.85 arcsec on the sky and delivered a FWHM spectral resolution of 10 km s^{-1}. Using the same detector as for the direct imaging and a slit-length of 163 arcsec, 640 spatial increments along the slit were obtained, each 0.255 arcsec long.

The 87th order containing [N II] λ6584 was isolated by means of a band-pass-type filter of 16-Å HPBW. Four offset spectra in this line, each with an exposure time of 1800 s, were obtained on 1993 June 4/5 UT. The slit-centre offsets from P Cyg for these exposures were 4 arcsec north, 2 arcsec north, 4.3 arcsec south and 8.3 arcsec south. The CCD frames were processed as described in Section 3, and Th–Ar arc spectra were used to perform wavelength calibration of the data. Particularly in the spectra taken closest to the star, a strong scattered stellar continuum passed through the spatial centre of the spectral images. This scattered continuum strip was removed from each long-slit spectrum using the scattered light distribution along the slit observed to either side of the wavelength range in which nebular line emission was apparent. Grey-scale position–velocity plots of the 4 arcsec north, 2 arcsec north and 4.3 arcsec south offset spectra are shown in Figs 4(a), (b) and (c) (opposite p. L32).

Inspection of Figs 4(a)–(c) reveals somewhat irregular shell-like structures. We measure projected expansion velocities of 118, 136 and 138 km s^{-1} at the 4 arcsec north, 2 arcsec north and 4.3 arcsec south slit positions, respectively, from one-half of the separation between the peaks of the emission close to the slit centre. Under the assumption that the observed emission arises from a simple expanding shell, these velocities deproject to 126, 139 and 150 km s^{-1}, respectively. We adopt a mean expansion velocity of 140 ± 10 km s^{-1} from the [N II] spectra. This expansion velocity is significantly larger than those measured for other LBV nebulae (e.g. Smith 1991; Smith, Crowther & Prinja 1994).

A bandpass filter of 70-Å HPBW centred at 7380 Å was used to isolate the 77th order to obtain [Ni II] λ7412 long-slit

spectra. Four 1800-s exposures were obtained on 1993 June 5/6, with the slit centre offset respectively 8 arcsec north, 6 arcsec north, 2 arcsec south and 6 arcsec south of P Cyg. The [Ni II] long-slit spectra were reduced in the same way as described for those of the [N II] line; grey-scale position–velocity displays of the 6 arcsec north, 2 arcsec south and 6 arcsec south offset spectra are shown in Figs 4(d), (e) and (f).

In the [Ni II] line, the shell structure has a finer, knottier appearance than that of the [N II] line. The brighter [Ni II] knots are characterized by sizes of about 2 arcsec and velocity FWHM of ~ 18 km s^{-1}. The [N II] velocity widths are a factor of 2 or more larger, consistent with the relative widths in the UES spectrum (Fig. 1). Following the same procedure as for [N II], we measure projected expansion velocities of 87, 106 and 98 km s^{-1} at the 6 arcsec north, 2 arcsec south and 6 arcsec south [Ni II] slit positions, respectively, which deproject to 103, 108 and 116 km s^{-1}. We adopt a mean expansion velocity of 110 ± 10 km s^{-1} from the [Ni II] spectra, 30 km s^{-1} less than that derived from the [N II] spectra.

A filter of 70-Å HPBW, tilted to give a central wavelength of 6725 Å, was used to isolate the [S II] $\lambda\lambda$6717, 6731 doublet lines in the 89th order. Due to the faintness of the [S II] lines (each having a flux of 34 on a scale where Hα is 285; JBDB), three exposures totalling 4600 s were obtained on 1993 June 12/13 at an offset position 8 arcsec north of P Cyg, along with two exposures totalling 3600 s obtained 5 arcsec north of the star. The long-slit spectra were reduced in the same manner as described above, and the relative fluxes of the two [S II] lines were calibrated with respect to observations of the stellar continuum of P Cyg. Due to the faintness of the lines, all the nebular emission along each slit position was extracted as a single spectrum. For the 8 arcsec north long-slit position, the integrated spectrum yielded an [S II] flux ratio $I(6717)/I(6731) = 1.22$, which, for the atomic parameters listed in Mendoza (1983), corresponds to $n_e = 875$ cm^{-3} for $T_e = 5000$ K, and $n_e = 1180$ cm^{-3} for $T_e = 10^4$ K. For the 5 arcsec north long-slit position, the integrated spectrum yielded three velocity components, with $I(6717)/I(6731) = 1.16$, 1.14 and 1.43 measured for the red, central and blue components, corresponding to $n_e = 700$–1000 cm^{-3} for the red and central components for T_e in the range 5000–10^4 K, and to $n_e = 1500$–2000 cm^{-3} for the blue component.

5 DISCUSSION

First, we estimate the mass of the bright inner nebula. The integrated [N II] λ6584 flux estimated in Section 2, together with the Hα-to-λ6584 ratio of unity derived by JBDB, implies an integrated Hα flux of 1.7×10^{-12} erg cm^{-2} s^{-1} from the inner nebula. For $E(B-V) = 0.60$, this corresponds to a dereddened Hα flux of 6.5×10^{-12} erg cm^{-2} s^{-1}, or $I(\mathrm{H}\beta) = 2.2 \times 10^{-12}$ erg cm^{-2} s^{-1} assuming Case B recombination ratios. The total nebular ionized mass M (assuming all hydrogen and helium to be ionized) is found from equation (5) of Barlow (1987) to be $M = 9.3 \times 10^{-3}\,\mathrm{M}_\odot$, where we have adopted $n(\mathrm{He})/n(\mathrm{H}) = 0.5$, as derived for P Cyg's wind by Barlow (1991), along with an electron temperature of 5000 K (following the discussion by JBDB) and an electron density of 1000 cm^{-3} (Section 4) for the emitting gas. A distance D of 1.8 kpc was also adopted (see below). The derived ionized nebular mass is at the bottom end of the range found for other LBV nebulae, and is about a factor of 300 smaller than the ionized masses of the AG Car and He 3-519 nebulae (Hutsemékers 1994; Smith et al. 1994).

For Case B recombination, our estimate of the dereddened Hβ flux from the inner nebula predicts a 5-GHz radio free–free flux of 4.1 mJy. It would be of interest to reprocess past Very Large Array (VLA) observations of P Cyg, particularly those obtained with the shortest baseline configurations, in order to look for evidence of nebular emission at this level surrounding the bright stellar wind radio source.

If the inner nebula is photoionized, the number of Lyman continuum photons that would be needed to maintain the ionization is 1.8×10^{45} s^{-1}. This would be comfortably within P Cyg's capabilities if it had no wind. The wind is very optically thick in the hydrogen Lyman continuum, however, its ionization being maintained by Balmer continuum photoionization from $n = 2$ (Drew 1985). The Lyman photon luminosity of the star therefore depends on the temperature and radius at the point where the wind finally becomes optically thin in the Lyman continuum, and cannot be estimated with any degree of accuracy as yet.

Hence the alternative scenario to consider is that the nebula is mainly ionized and excited by shocks. It seems inevitable that shocks must occur. The nebular knots are moving out at a velocity of 110–140 km s^{-1}, while P Cyg's wind currently has a velocity of between 206 km s^{-1} (from the UV Fe II absorption lines: Lamers, Korevaar & Cassatella 1985) and 220 km s^{-1} (from the on-star [Ni II] linewidths: Section 2), although the stellar wind velocity could have been lower in the past. Our interpretation of the data is that the observed [N II] emission originates from fairly dense compact knots which are moving outwards at ~ 110 km s^{-1} and are being overtaken by the stellar wind at a relative velocity of ~ 100 km s^{-1}. The low ionization potential of Ni (7.635 eV) allows significant [Ni II] emission to originate from the knot cores without accompanying [N II] emission (the ionization potential of N is 14.534 eV). However, significant [N II] emission is produced by shocked wind material in bow shocks around the clumps (see table 3 of Hartigan, Raymond & Hartmann 1987), with much larger velocity widths due to the large line-of-sight velocity range of the shocked wind material flowing round the obstacle.

Following Hartigan et al. (1987), the FWZI of an individual velocity component, corrected for instrumental and thermal broadening, is predicted to be equal to the velocity of the shock impacting the knot. The full widths measured for the two brightest features seen in the 4 arcsec north [N II] spectrum (Fig. 4a) are 127 and 138 km s^{-1}; while, for the brightest blobs in each of Figs 4(b) and (c) (2 arcsec north and 4.3 arcsec south), the full widths are 104 and 80 km s^{-1}; and, for the two brightest blobs in our 8.3 arcsec south [N II] spectrum (not shown), the full widths were measured to be 66 and 119 km s^{-1}. Allowing for the estimated measurement errors of ± 15 km s^{-1} and the instrumental resolution of 10 km s^{-1}, these widths are consistent with mean bow shock velocities of ~ 100 km s^{-1}. Smaller linewidths are measured for the [Ni II] knots – the two brightest features in Fig. 4(d) (6 arcsec north) have FWZIs of 47 and 55 km s^{-1}, while a full

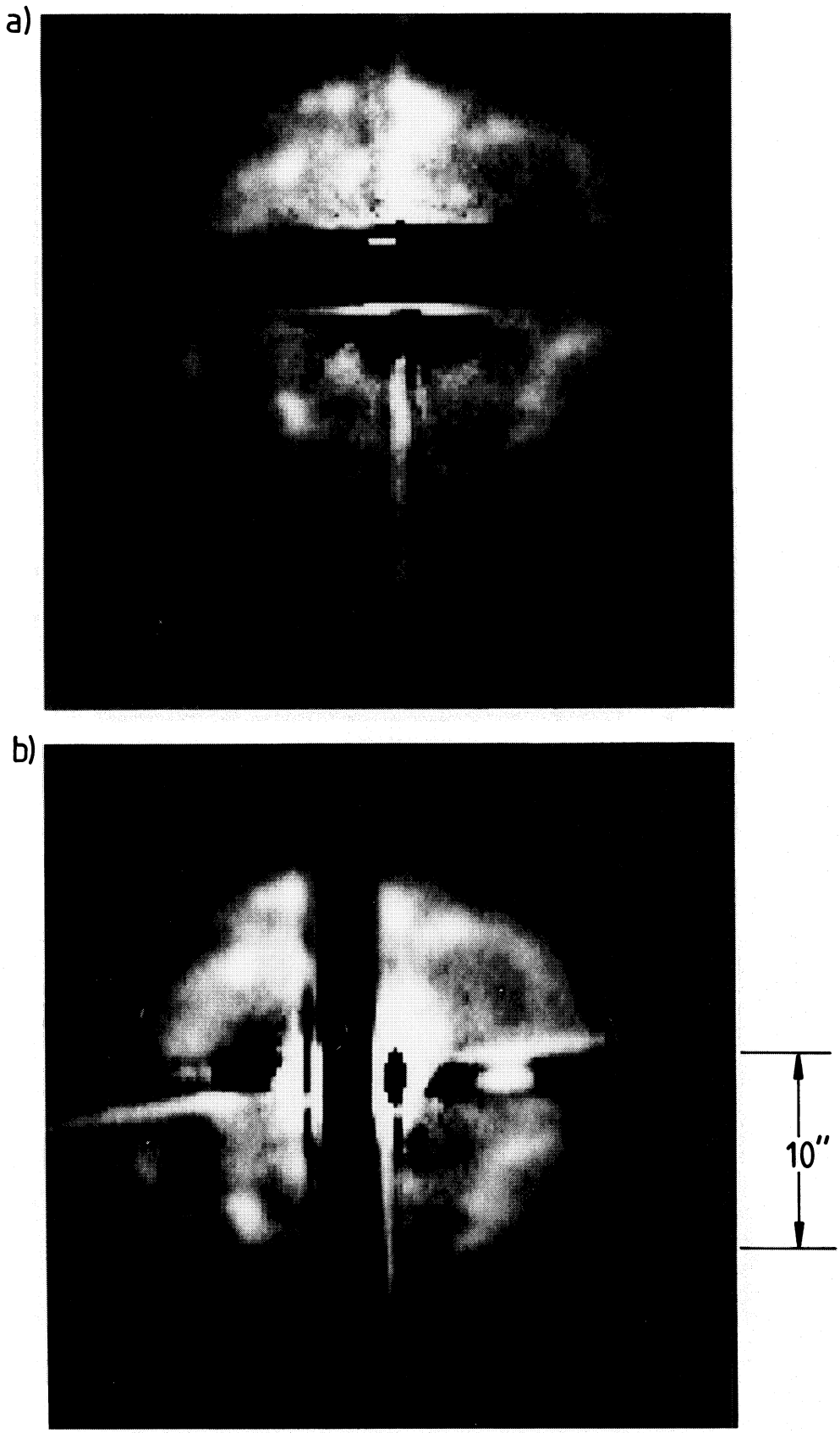

Figure 2. Images of the inner nebula in the [N II] 6584-Å line. North is at the top and east is to the left in both images. The images in (a) and (b) were obtained with the 4.3 arcsec wide occulting strip oriented east–west and north–south, respectively, and the broad dark band in each panel is due to the occulting strip. There are also occulted stripes at 90° to the occulting strip orientation, due to the telescope diffraction spikes. The beading along their length combines with minor misalignments between the broad-band and narrow-band images to produce alternating bright and dark regions in their place after subtraction.

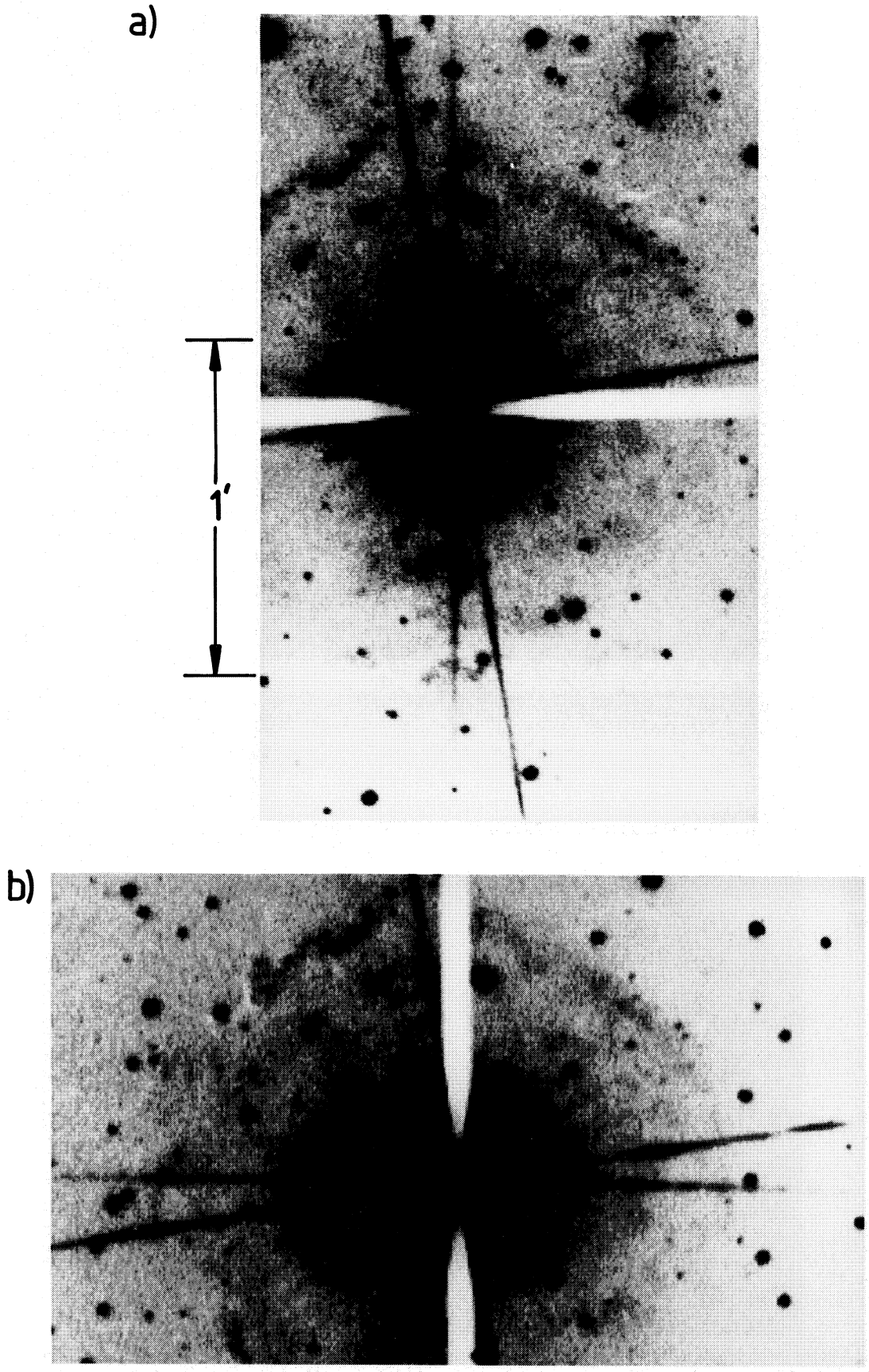

Figure 3. Negative grey-scale images of the outer nebulosity in the [N II] 6584-Å line are shown. The images in (a) and (b) were obtained with the 4.3 arcsec wide occulting strip oriented east–west and north–south, respectively. No continuum subtraction has been applied. The occulting strip is here seen as a white stripe, and the diffraction spikes appear as dark straight lines.

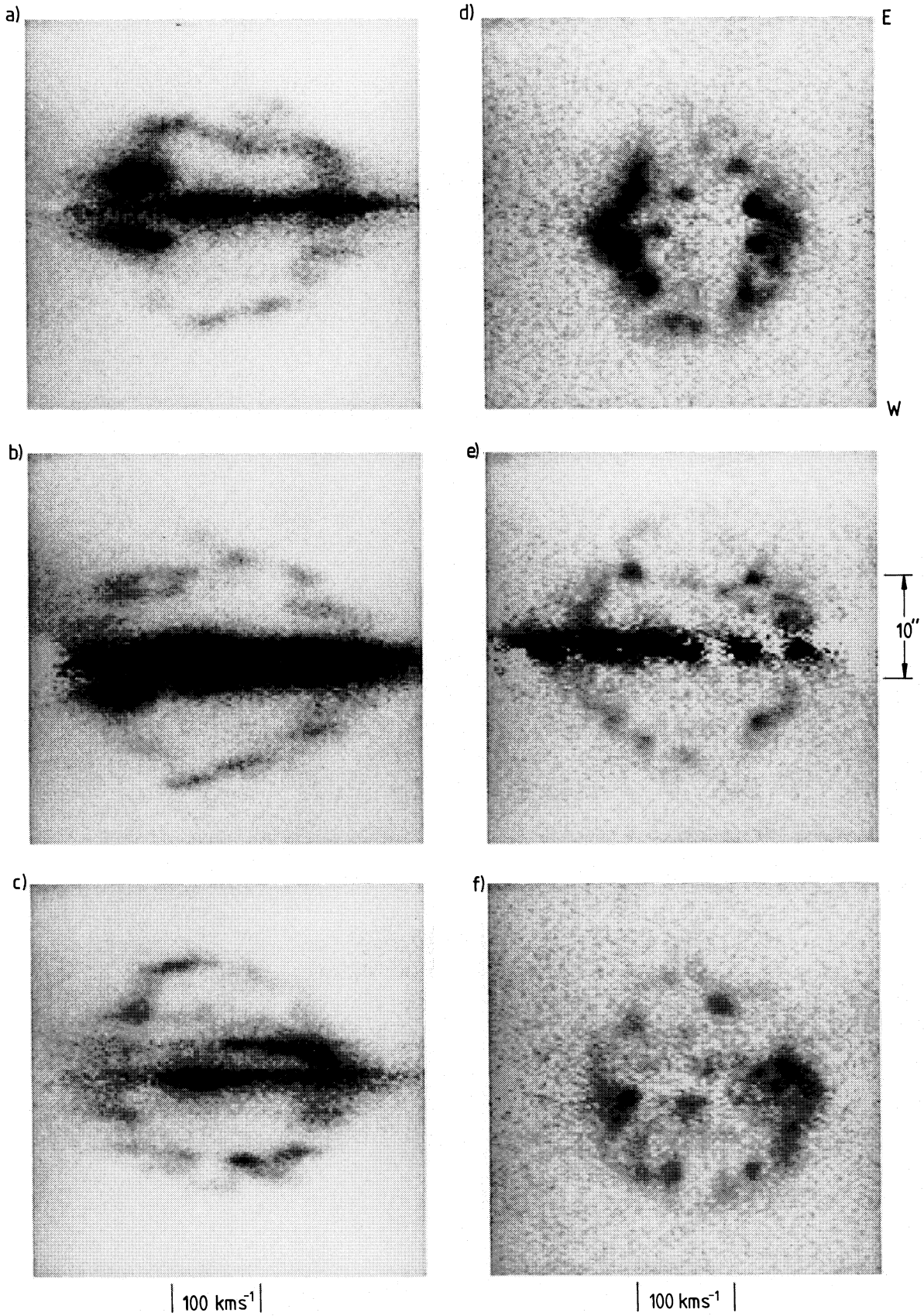

Figure 4. Negative grey-scale representation of the [N II] 6584-Å long-slit spectra obtained 4 arcsec north, 2 arcsec north and 4.3 arcsec south of P Cyg are shown in panels (a), (b) and (c) respectively. Those for [Ni II] 7412 Å obtained 6 arcsec north, 2 arcsec south and 6 arcsec south are shown in (d), (e) and (f) respectively. The spectrum of the scattered stellar light has been subtracted in all cases. The dark horizontal bands, particularly obvious in the 2 arcsec offset spectra, are the residuals of this process.

width as small as 17 km s^{-1} is measured for one feature in our 8 arcsec north [Ni II] spectrum. Although the full width of a bow shock emission line should be independent of the viewing angle ϕ (Hartigan et al. 1987), its radial velocity centroid will have a viewing-angle-dependent offset from that of the obstacle causing the shock. For a line of sight perpendicular to the radius vector between the star and the clump ($\phi = 90°$), there will be no radial velocity offset between the bow shock emission and the clump, while for $\phi = 0°$ (i.e. viewing along the star–clump radius vector) the bow shock emission is predicted to be shifted by -50 km s^{-1} for near-side clumps and by $+50$ km s^{-1} for far-side clumps, in the case of a 100 km s^{-1} shock. From figs 3(i)–(l) of Hartigan et al. (1987), a mean velocity offset of 25–40 km s^{-1} is expected for an ensemble of bow shocks observed with a mean viewing angle of 45°, consistent with the 30 km s^{-1} larger expansion velocity found for [N II] compared to [Ni II] (Section 4), provided that the [Ni II] emission originates from within the clumps while the [N II] emission originates from the bow shocks.

If the [Ni II] emission arises from dense clumps, this would also resolve the problem of the large [Ni II] relative line strengths that are observed, since the Hα, [Ni II] and [S II] lines would all originate from ionized material in the bow shocks around the clumps, while the [N II] emission would arise from mainly neutral material inside the clumps. Although sulphur has an ionization potential of only 10.26 eV, the [S II] 6717, 6731-Å lines would be collisionally suppressed at $n_e \sim 10^6$ cm^{-3} and should be excited only in the shocked stellar wind downstream of the bow shock, consistent with its observed linewidths which are similar to those of [N II] λ6584. The current mass-loss rate of 2.2×10^{-5} $M_\odot$ yr^{-1} from P Cyg (Barlow 1991) should give a pre-shock density of 17 cm^{-3} at the edge of the bright inner nebula. For a pre-shock wind temperature of 5×10^3–10^4 K, corresponding to a sound velocity of ~ 6 km s^{-1}, a 100 km s^{-1} shock would give a final downstream density of ~ 5000 cm^{-3} for the shocked wind material, consistent with the electron density range of 700–2000 cm^{-3} yielded by the observed [S II] doublet ratios. The solar-abundance bow shock models of Hartigan et al. (1987) predict no [O III] λ5007 emission for shock velocities of 80 km s^{-1} or less – the λ5007 dereddened relative intensity of 110 seen in our offset UES spectrum is consistent with their models for shock velocities of ~ 100 km s^{-1}. In addition to the above considerations, mass-loading of the post-shock flow could occur, if material were ablated from the clumps (Hartquist et al. 1986).

The nebulae around other Galactic LBVs all exhibit strong dust emission (Hutsemékers 1994). We can scale the observed *IRAS* 60-μm fluxes from these nebulae by the ratio of the dereddened nebular Hα flux from the P Cygni nebula (estimated above) to those of the other nebulae (the latter tabulated by Hutsemékers 1994), to predict the 60-μm flux expected from the P Cygni nebula for the same ratio of dust to ionized gas. A scaling of the dust emission from the AG Car and He 3-519 nebulae would predict 7–8 Jy at 60 μm from the P Cygni nebula, while scaling of the emission from He 3-591 (WRA 751) and HR Car would predict 16 and 37 Jy, respectively. The *IRAS* Point Source Catalog yields a colour-corrected flux of 2.4 Jy at 60 μm from P Cyg, while Waters & Wesselius (1986) noted a rapidly varying background and obtained 2.05 Jy by co-adding many individual *IRAS* scans, corresponding to an excess of only ~ 0.5 Jy above the expected free–free emission from the stellar wind at this wavelength. A pointed *IRAS* DPP observation of P Cyg obtained by one of us (MJB) yielded a 60-μm flux of 1.5 Jy (Deacon 1991), corresponding to no excess over the expected wind emission. We therefore conclude that the nebula around P Cygni contains much less dust than do the nebulae around other Galactic LBV stars. If no depletion of nickel on to grains has occurred in the P Cygni nebula, this would also help to explain the great strength of its [Ni II] lines.

To obtain an age estimate for the bright inner nebula of P Cygni, we adopt a mean angular radius of 11.3 arcsec (Section 3), a distance of 1.8 kpc to P Cyg (based on its proposed membership of the open cluster IC 4996: van Schewick 1968; Lamers, de Groot & Cassatella 1983) and a nebular expansion velocity of 110 km s^{-1} from the [Ni II] line (see above), assumed to have remained constant over time. These imply a nebular expansion age of 880 yr, over twice the time that has elapsed since P Cyg's great outburst of 1600 AD. If we wish to associate the inner nebula with this event, a distance to P Cyg of just 0.8 kpc will be required. For an $E(B-V)$ of 0.60 (Barlow & Cohen 1977; Lamers et al. 1983; Deacon & Barlow 1991), this distance would imply an absolute visual magnitude of -6.6 for P Cyg, versus -8.3 for a distance of 1.8 kpc. The former would be unexceptional for an early B supergiant, and quite inconsistent with the hypergiant status implied by the extreme mass-loss characteristics of P Cyg's spectrum. Nothing is known of this star's photometric history prior to its discovery in 1600 AD (de Groot 1969), so the possibility that the 11.3 arcsec radius nebula was ejected ~ 900 yr ago cannot be excluded. An image that we obtain through the [Ni II] filter with an exposure time of only 50 s hints at the presence of two inner nebular rings, with radii of ~ 11 and ~ 6 arcsec. In our [Ni II] spectrum shown in Fig. 4(e) (2 arcsec south), there are features located at about 6 arcsec east and west of the slit centre that could correspond to a partial 6 arcsec radius shell, while blobs in the centre of the 6 arcsec north and south slits (Figs 4d and f) could correspond to the edges of such a shell. These observations require confirmation but, if real, a ~ 6 arcsec radius shell could date back to *circa* 1600 AD. The existence of the faint outer nebular shells (Fig. 3) implies past episodic mass ejections. The measurement of expansion velocities for these outer shells could allow them to be dated to construct an outburst history for the star.

ACKNOWLEDGMENTS

We thank Bill Garner for his skill in printing the images. We take this opportunity to record our debt to the enthusiasm of Dean Johnson and the response of Elias Brinks that led to the observations of JBDB and prompted this study. JED acknowledges an SERC Advanced Fellowship.

REFERENCES

Baars J. W. M., Wendker H. J., 1987, A&A, 181, 210
Barlow M. J., 1987, MNRAS, 227, 161
Barlow M. J., 1991, in van der Hucht K. A., Hidayat B., eds, Proc. IAU Symp. 143, Wolf-Rayet Stars and their Interrelations with other Massive Stars in Galaxies. Kluwer, Dordrecht, p. 281

Barlow M. J., Cohen M., 1977, ApJ, 213, 737
Clampin M., Nota A., Golimowski D. A., Leitherer C., Durrance S. T., 1993, ApJ, 410, L35
Conti P. S., 1984, in Maeder A., Rensini A., eds, Observational Tests of the Stellar Evolution Theory. Reidel, Dordrecht, p. 233
Davidson K., Dufour R. J., Walborn N. R., Gull T. R., 1986, ApJ, 305, 867
Davidson K., Moffat A. F. J., Lamers H. J. G. L. M., eds, 1989, Physics of Luminous Blue Variables. Kluwer, Dordrecht
Deacon J. R., 1991, PhD thesis, University of London
Deacon J. R., Barlow M. J., 1991, in van der Hucht K. A., Hidayat B., eds, Proc. IAU Symp. 143, Wolf-Rayet Stars and their Interrelations with other Massive Stars in Galaxies. Kluwer, Dordrecht, p. 558
de Groot M., 1969, Bull. Astron. Inst. Neth., 20, 225
Drew J. E., 1985, MNRAS, 217, 867
Hartigan P., Raymond J., Hartmann L., 1987, ApJ, 316, 323
Hartquist T. W., Dyson J. E., Pettini M., Smith L. J., 1986, MNRAS, 221, 715
Humphreys R. M., 1989, in Davidson K., Moffat A. F. J., Lamers H. J. G. L. M., eds, Physics of Luminous Blue Variables. Kluwer, Dordrecht, p. 3
Hutsemékers D., 1994, A&A, 281, L81
Johnson D. R. H., Barlow M. J., Drew J. E., Brinks E., 1992, MNRAS, 255, 261 (JBDB)
Lamers H. J. G. L. M., de Groot M., Cassatella A., 1983, A&A, 128, 299
Lamers H. J. G. L. M., Korevaar P., Cassatella A., 1985, A&A, 149, 29
Leitherer C., Zickgraf F. J., 1987, A&A, 174, 103
Meaburn J., Blundell B., Carling R., Gregory D. F., Kerr D., Wynne C. G., 1984, MNRAS, 210, 463
Mendoza C., 1983, in Flower D. R., ed., Proc. IAU Symp. 103, Planetary Nebulae. Reidel, Dordrecht, p. 143
Mitra P. M., Dufour R. J., 1990, MNRAS, 242, 98
Nota A., Leitherer C., Clampin M., Greenfield P., Golimowski D. A., 1992, ApJ, 398, 621
Nussbaumer H., Storey P. J., 1982, A&A, 110, 295
Smith L. J., 1991, in van der Hucht K. A., Hidayat B., eds, Proc. IAU Symp. 143, Wolf-Rayet Stars and their Interrelations with other Massive Stars in Galaxies. Kluwer, Dordrecht, p. 385
Smith L. J., Crowther P. A., Prinja R. K., 1994, A&A, 281, 833
Stahl O., Wolf B., 1986, A&A, 158, 371
van Schewick H., 1968, Z. Astrophys., 68, 229
Walborn N. R., 1982, ApJ, 256, 452
Waters L. B. F. M., Wesselius P. R., 1986, A&A, 155, 104
Wendker H. J., 1982, A&A, 116, L1